Advances in Environmental Research, *Vol. 3*, *No. 3* (*2014*) *231-251*
DOI: http://dx.doi.org/10.12989/aer.2014.3.3.231

Modelling and packed bed column studies on adsorptive removal of phosphate from aqueous solutions by a mixture of ground burnt patties and red soil

Prangya R Rout [a], Rajesh R Dash [*] and Puspendu Bhunia [b]

Department of Civil Engineering, School of Infrastructure, Indian Institute of Technology, Bhubaneswar - 751 013, Odisha, India

(*Received April 01*, *2014*, *Revised July 09*, *2014*, *Accepted July 21*, *2014*)

Abstract. The present study examines the phosphate adsorption potential and behavior of mixture of Ground Burnt Patties (GBP), a solid waste generated from cooking fuel used in earthen stoves and Red Soil (RS), a natural substance in fixed bed column mode operation. The characterization of adsorbent was done by Proton Induced X- ray Emission (PIXE), and Proton Induced γ- ray Emission (PIGE) methods. The FTIR spectroscopy of spent adsorbent reveals the presence of absorbance peak at 1127 cm^{-1} which appears due to $P = O$ stretching, thus confirming phosphate adsorption. The effects of bed height (10, 15 and 20 cm), flow rate (2.5, 5 and 7.5 mL/min) and initial phosphate concentration (5 and 15 mg/L) on breakthrough curves were explored. Both the breakthrough and exhaustion time increased with increase in bed depth, decrease in flow rate and influent concentration. Thomas model, Yoon-Nelson model and Modified Dose Response model were used to fit the column adsorption data using nonlinear regression analysis while Bed Depth Service Time model followed linear regression analysis under different experimental condition to evaluate model parameters that are useful in scale up of the process. The values of correlation coefficient (R^2) and the Sum of Square Error (SSE) revealed the Modified Dose Response model as the best fitted model to the experimental data. The adsorbent mixture responded effectively to the desorption and reusability experiment. The results of this finding advocated that mixture of GBP and RS can be used as a low cost, highly efficient adsorbent for phosphate removal from aqueous solution.

Keywords: phosphate adsorption; ground burnt patties; red soil; modified dose response model; Yoon-Nelson model; thomas model; BDST model

1. Introduction

Phosphorus is an essential chemical element, widely used in many industrial, agricultural, environmental and household applications. It naturally exists in the form of phosphate, which is a vital nutrient for the growth of plants, animals and microorganisms in most of the ecosystems. Due to its low concentration occurrence in the environment, it usually serves as the limiting nutrient

*Corresponding author, Assistant Professor, E-mail: rrdash@iitbbs.ac.in
[a] M.Tech., E-mail: prr10@iitbbs.ac.in
[b] Ph.D., E-mail: pbhunia@iitbbs.ac.in

http://www.techno-press.org/?journal=aer&subpage=7 ISSN: 2234-1722 (Print), 2234-1730 (Online)

(Huang *et al.* 2013a). On the other hand, with the fast progress of modern economy, the excess discharge of phosphates is taking place through various human activities such as the use of fertilizers, industrial and domestic wastewater discharge, rural and urban sewage disposal, etc. The increasing inputs of phosphates to aquatic environments lead to increased rates of eutrophication, thereby jeopardizing the quality of domestic, industrial, agricultural and recreational water resources (Jia *et al.* 2013). The consequences of eutrophication include algal bloom, low dissolved oxygen, murky water, depletion of desirable flora and fauna, ecological imbalance in aquatic ecosystems and the production of microsystin, an environmental toxin that cause hepatocellular carcinoma in humans (Yuan *et al.* 2006). In order to control eutrophication, total phosphorous concentration in natural water bodies should be less than 0.10 mg *P*/*L* (Nur *et al.* 2013). To meet the stringent limit of phosphorous concentration in natural water bodies, the discharge standard of wastewater containing phosphorus is on an average set at 1-2 mg *P*/*L* (Huang *et al.* 2013b). Removal of phosphate from wastewater is therefore of great importance before their discharge into natural water bodies.

A number of methods for phosphate abatement have been explored, including physical processes, chemical precipitation, biological treatment and adsorption based processes, etc. Of the various processes, adsorption with the advantage of high removal efficiency, operation simplicity, invulnerability to coexisting pollutants, economical and less sludge production has attracted immense interest (Zong *et al.* 2013). The proficiency of the adsorption process depends upon the adsorbent materials, which should have the property of low cost, easy availability and high uptake capacity. The most lucrative materials are usually found among various natural and waste materials (Mateus *et al*. 2012). A number of natural materials like various soils, laterite, andensite, granite, etc. and waste materials like refuse concrete, waste paper, mussel shell, limestone waste; used bricks, coir pith, corn residues, etc. have been reported as efficient adsorbents to reduce phosphorous concentrations in the effluents (Ioannou *et al*. 2013, Kadam *et al*. 2009, Zhang *et al*. 2011, Rahaman *et al*. 2005, Chen *et al*. 2012, Jia *et al*. 2013, Krishna and Haridash 2008, Wang *et al*. 2008). In the present study the phosphate adsorption potential and behavior of mixture of Ground Burnt Patties (GBP), a solid waste generated from cooking fuel used in earthen stoves and Red Soil (RS), a natural substance has been examined in a packed bed column. The same authors have demonstrated the use of RS (Rout *et al*. 2014a) and grounded GBP (Rout *et al*. 2014b) as potential adsorbents for phosphate removal from wastewater through batch mode of operation. It was observed that the phosphate adsorption capacities of both the novel adsorbents, RS and GBP are equally good. But the permeability of RS is low due to its fine particular nature where as GBP has shown higher hydraulic conductivity due to its porous granular nature. So GBP can be mixed with RS to achieve enhanced permeability and hydraulic conductivity of treatment systems.

Batch adsorption data are more appropriate for small scale treatment volumes, but inconvenient in the case of large scale treatment volumes due to overestimation of sorption capacities. In order to obtain more realistic laboratory results, the fixed bed column study is essential, since it has a greater resemblance to the flow conditions in full scale constructed filters. Moreover, continuous flow experiments are significant to predict the column breakthrough, which determines the functional life span of the column bed (Mateus and Pinho 2010). In continuation of the previous batch studies (Rout *et al*. 2014a, b), the present paper deals with the performance evaluation of mixture of RS and GBP for phosphate removal from aqueous solution in fixed bed column mode of operation. The mixture of both the adsorbents has been considered to prevent possible clogging problem that may arise due to aggregation of RS in the water phase, to maintain higher hydraulic conductivity and to achieve efficient phosphate removal. The effects of flow rate, bed height and

initial phosphate concentration, on breakthrough curves were examined. The experimental data were validated by various extensively used column adsorption models like bed-depth service time (BDST), Thomas Model, Yoon–Nelson Model (Y-N Model) and Modified Dose Response Model (MDR Model). The adequacy of the models was evaluated by calculating the percentage errors between the experimental and predicted values. The performance of the fixed bed column in treating phosphate containing real wastewater was also assessed. Regeneration study was undertaken to explore reusability of the adsorbents.

2. Materials and methods

2.1 Adsorbent

GBP were collected from different waste disposal sites of Bhubaneswar city, and RS was collected from the Balibagada village area in Ganjam district of Odisha, India. Both the adsorbents were washed several times with distilled water to remove surface adhered particles, soluble materials and dried in hot-air oven at 100°C for overnight. Subsequently the adsorbents were grounded, sieved and particle sizes of less than 0.3 mm were used as adsorbents in the adsorption study. The properties and average chemical composition of both the material were given in Table 1. For the composition analysis of GBP and RS, highly sensitive multi component analytical methods like Proton Induced X- ray Emission (PIXE) and Proton Induced γ-ray Emission (PIGE) were used.

2.2 Adsorbate

Phosphate stock solution of 1000 mg L^{-1} was prepared by dissolving 4.388 g of analytical grade anhydrous potassium dihydrogen phosphate (KH_2PO_4) in 1 L distilled water. The stock solution was further diluted to get the desired concentrations of experimental working solution. This synthetic phosphate solution was used for optimizing different adsorption parameters in column studies.

2.3 Analytical methods

The chemical compositions of the adsorbents were analyzed with the help of Proton Induced γ-ray Emission (PIGE) and Proton Induced X- ray Emission (PIXE). Measurements were carried out using the 2 MeV proton beam obtained from 3 MV Tandem pelletron accelerator. In order to get better resolution and clarity of results, PIXE was done for analysis of elements with atomic number as low as 12 (low Z elements) and PIGE was done for analysis of high Z elements following the method as described by Kennedy *et al*. (1999). The specific surface area of the adsorbents determined by the BET nitrogen gas sorption method using a specific surface area analyzer (Gemini2360, Micromeritics, USA). pH_{zpc} of the adsorbents were measured following pH drift method (Ioannou *et al*. 2013).

Vanado molybdo phosphoric acid method (4500-P) was followed to analyze phosphate according to standard methods for the examination of water and wastewater (APHA 2005). Vanadate-molybdate reagent of 1 mL and 0.5 mL of distilled water were added to 3.5 mL of filtered sample. The mixed solution was analyzed after 10 min with a Perkin Elmer Lambda-25 UV/VIS spectrophotometer at the detection wavelength of 470 nm. pH_{zpc} of the adsorbent was

measured following pH drift method (Ioannou *et al*. 2013).

2.4 FTIR studies

Infrared spectra of pure and phosphate adsorbed adsorbents were obtained using a Bruker ALPHA-FTIR Spectrophotometer. Samples were prepared in KBr disks (2 mg sample in 200 mg KBr). The scanning range was 500-4000 cm^{-1} and the resolution was 2 cm^{-1} with a scanning rate of 16. Spectra of both the adsorbents before and after phosphate adsorption were recorded.

2.5 Fixed bed column studies

A column having an inner diameter of 4.5 cm and height 50 cm, made up of the transparent polyacrylic sheet was used in this study. It has openings at different bed heights of 10, 15 and 20 cm for collection of samples At the bottom of the column a polyacrylic sieve was attached followed by glass wool to provide support and to prevent the loss of adsorbent materials. The column was filled with the adsorbents and the bed was washed by passing distilled water through it. The phosphate removal studies were conducted in the down flow column reactor with synthetic phosphate solutions of different concentrations (5 and 15 mg L^{-1}) and varying velocities (1.5, 3 and 4.5 mL min^{-1}) in a continuous mode using a peristaltic pump (Miclins VSP-200-2C). Neutral pH and 25 ± 2°C temperatures was maintained for the influent solution. Periodic monitoring and data collection was carried out at regular interval of 1 h to obtain the breakthrough time, breakthrough curve, exhaustion curve, etc., which ultimately determine the operation and dynamic response of the adsorption column. The breakthrough time (t_b) in this study represents the time corresponding to 93.5% removal of phosphates (80.5% for initial Phosphate concentration of 5 mg/L), i.e., effluent phosphate concentration less than 1 mg/L whereas, exhaust time (t_e) signifies the time matching to 5% removal of phosphate.

2.6 Analysis of column design parameters

The data obtained from column studies was used to get the breakthrough curve by plotting C_t/C_0 (the ratio of effluent and influent phosphate concentration) vs. time (t). The quantity of total phosphate adsorbed in the column (q_{total}) is calculated from the area under the breakthrough curve by using the following formula (Chen *et al*. 2012)

$$q_{total} = \frac{Q}{1000}\int_{t=0}^{t=total} C_r dt \tag{1}$$

where Q is the volumetric flow rate (L/h) and $C_r = C_0 - C_t$, is the phosphate removal (mg/L) concentration.

The equilibrium phosphate uptake capacity of the column, q_{eq} (mg/g), is calculated as the following

$$q_{eq} = \frac{q_{total}}{m} \tag{2}$$

where m is the weight of the adsorbent in the column (g).

The total amount of phosphate entering the column (P_{total}) can be found out with the help of the

equation given below

$$P_{total} = \frac{C_0 Q t_e}{1000} \tag{3}$$

where t_e = exhaustion time (h).

The removal percentage of phosphate (R) can be achieved through the following equation

$$R(\%) = \frac{q_{total}}{P_{total}} \times 100 \tag{4}$$

The mass transfer zone (*MTZ*), which is the length of the adsorption zone in the column, indicates the efficiency in the use of adsorbents in the column. *MTZ* (cm) can be calculated as follows (Adak *et al*. 2006)

$$MTZ = L\left(\frac{t_e - t_b}{t_e}\right) \tag{5}$$

where, L = length of the adsorbent in the column (cm) and t_b = breakthrough time (h).

The time required for the *MTZ* to move the length of its own height up/down the column is represented by t_z and can be calculated as mentioned in the equation below

$$t_z = \frac{V_e - V_b}{Q} \tag{6}$$

where, $V_e = Qt_e$, total effluent volume up to exhaustion time (L) and $V_e = Qt_b$, total effluent volume up to breakthrough time (L).

The rate at which *MTZ* is moving up/down through the adsorbent bed is denoted by U_z (cm/h) and can be expressed as

$$U_z = \frac{MTZ}{t_z} \tag{7}$$

The time of contact between the water phase and the adsorbent is termed as Empty Bed Contact Time (*EBCT*). *EBCT* (min) basically measures the critical depth and the contact time for an adsorbent. It can be calculated as per the following equation

$$EBCT = \frac{V}{Q} \tag{8}$$

where, V = adsorbent bed volume (mL).

In case of a symmetric breakthrough curve, the time taken by the effluent concentration to reach half of the initial concentration is called stoichiometric time (t_s) (Cavas *et al*. 2011). The t_s for unsymmetrical breakthrough curves can be calculated from Eq. (9)

$$t_s = \frac{1}{C_0}\int_{t=0}^{t=te} C_r dt \tag{9}$$

Length of Unused Bed (*LUB*) is the length of the *MTZ* which remains unutilized even after the appearance of the exhaustion time of the bed. The *LUB* (cm) can be determined from the breakthrough curve according to the following equation (Chen *et al*. 2013)

$$LUB = L\left(\frac{t_s - t_b}{t_s}\right) \tag{10}$$

where, t_s is the time at which $C_t / C_0 = 0.5$ (for a symmetrical breakthrough curve).

2.7 Modelling of column adsorption data

Successful design of a fixed bed adsorption column necessitates the prediction of the concentration-time profile from the breakthrough curves. In order to envisage and analyze the dynamic behavior of phosphate adsorption onto the mixture of RS and GBP several models including BDST, Thomas, Yoon-Nelson and Modified dose-response models were applied to the experimental data. In order to find the best fit model, error analysis was done by considering the sum of the squares of the differences between the experimental data and the predicted data (data obtained by calculating from models). Sum of the Squares of Error (SSE) can be obtained as the following formula

$$\text{SSE} = \frac{\sum\left(\left(\frac{C_t}{C_0}\right)_c - \left(\frac{C_t}{C_0}\right)_e\right)^2}{N} \tag{11}$$

where, $(C_t / C_0)_c$ is the ratio of effluent and influent phosphate concentration obtained from the model calculation, $(C_t / C_0)_e$ is the ratio of effluent and influent phosphate concentration obtained from the experiment and N is the total number of experimental point.

3. Results and discussion

3.1 Characterization of adsorbent

The highly sophisticated experimental techniques such as PIXE and PIGE are engaged in the precise determination of elemental composition of GBP as well as RS. The major basic constituents of the adsorbents are given in Table 1. The presence of Al, Fe, Mg and CA-oxides are known to play an important role in phosphate removal (Yang *et al*. 2009). In spite of being the major component of both GBP and RS, the Si - oxide has a very insignificant role in phosphate removal (Johansson and Gustafsson 2000). Phosphate ions react with Fe and Al-oxides by ligand exchange forming inner-sphere complexes whereas the presence of Mg and Ca ion facilitates phosphate removal via precipitation (Lindsay 1979, Chen *et al.* 2007, Chimenos *et al*. 2003). The complete characterization of adsorbents and the adsorption process with the help of Fourier Transferred Infra-Red spectroscopy (FTIR), X-Ray Diffraction (XRD) and Scanning Electron Microscopy (SEM) have already been discussed in our published (Rout *et al.* 2014a, b) and unpublished works.

Table 1 Properties and compositions of GBP and RS

Properties and compositions	GBP	Red Soil
Particle size (mm)	< 0.3	< 0.3
pH zpc	8.62	7.51
BET surface area (m^2/g)	19.07	25.55
Bulk density (g/cm^3)	2.0	2.25
Porosity (%)	74.48	47.12
Specific gravity	2.41	4.51
Specific yield (%)	62.19	15.37
Specific retention (%)	12.29	31.75
SiO_2 (%)	52.71-54.49	52.45-54.3
Fe_2O_3 (%)	17.95-18.72	24.21-24.73
Al_2O_3 (%)	20.74-21.42	21.38-22.17
MgO (%)	4.85-5.01	4.85-5.01
Na_2O (%)	0.37-0.40	0.46-0.49
CaO (%)	3.8-4.11	0.31-0.34

3.2 FTIR studies

Adsorption process is highly influenced by the presence of different functional groups. To figure out the presence of $P = O$ bonds in the spectra of adsorbent after phosphate adsorption, the FTIR study was undertaken. The adsorbents before and after adsorption were termed as GBP, RS and GBPT, RST respectively. The infrared spectra of both the adsorbents before and after adsorption are shown in the Fig. 1, indicating the changes in the functional groups and surface properties of the adsorbents. The spectrum reveals the complex nature of the adsorbent process as evidenced by the presence of a large number of peaks. The infrared absorption between 1250 and 850 cm^{-1} corresponds to the stretching frequency region of phosphate species (Zheng *et al*. 2012).

The absorption peaks as determined by e-FTIR software, around 1127, 1173.5 and 1199.36 cm^{-1} in case of GBPT and around 1054.23, 1,127, and 1143.45 cm^{-1} in case of RST indicate the participation of $P = O$ entities in adsorption process, which is in agreement with the findings reported earlier (Elzinga and Sparks 2007). As a consequence, the above mentioned peaks were not present before phosphorous exposure, indicating absence of these functionalities in native adsorbent like GBP and RS. Well established investigational results by past researchers revealed that the frequency at 1126 cm^{-1} is mainly due to adsorption of $H_2PO_4^-$ resulting in $P = O$ stretch (Elzinga and Sparks 2007, Liana *et al*. 2010). Thus, the frequency appearing at 1127 cm^{-1} in this study is possibly due to the $P = O$ stretch as a result of adsorbed $H_2PO_4^-$. The slight difference in our experimental value and other additional peaks in the frequency ranges may arise due to the presence of different mineral phases within the native adsorbents. The FTIR spectra of spent adsorbent revealed the presence of peaks corresponding to $P = O$ stretch. Thereby confirming phosphate adsorption.

3.3 Fixed bed column studies

3.3.1 Preliminary experiments

Some of the flow through column experiments were performed prior to the main experiment to figure out the best alternative for phosphate removal. First of all both the adsorbents were taken separately in different columns with varying bed heights and the phosphorous removal ability of all the alternatives was explored. It was observed that, RS though efficient in phosphate removal, could aggregate in the water phase, decreasing hydraulic conductivity that ultimately leads to clogging of the bed in the long run. The observation is in agreement with the experimentally found properties of RS such as low porosity of bed, low specific yield and high retention time. On the other hand GBP columns, though equally potential in phosphate removal, gets saturated quickly due to comparatively high porosity in bed (74.48%), high specific yield (62.19%) and low retention capacity (12.29%) which eventually contribute to high hydraulic conductivity. In order to improve the permeability of the column, reduction of possible clogging problem, enhanced phosphate removal and for reducing the speed of attaining bed saturation time, the mixture of RS and GBP as adsorbents in fixed bed columns have been attempted. Different combinations (V/V) of RS and GBP such as 1:3, 1:5, 1:1, 2:3, 3:5 etc. were tested for the best feasible combination. During preliminary experiments, it was established that, out of multiple alternatives, the flow through column having 1:1 V/V combination of RS and GBP was capable of delivering consistent phosphate removal for longer duration of time maintaining good hydraulic conductivity. Therefore, this particular combination (1:1 (V/V) RS: GBP) of adsorbents mixture was used for the rest of the experiments.

Different column adsorption parameters on phosphate removal were examined. The fixed bed column adsorption experiments were performed at various bed depths, flow rates and influent

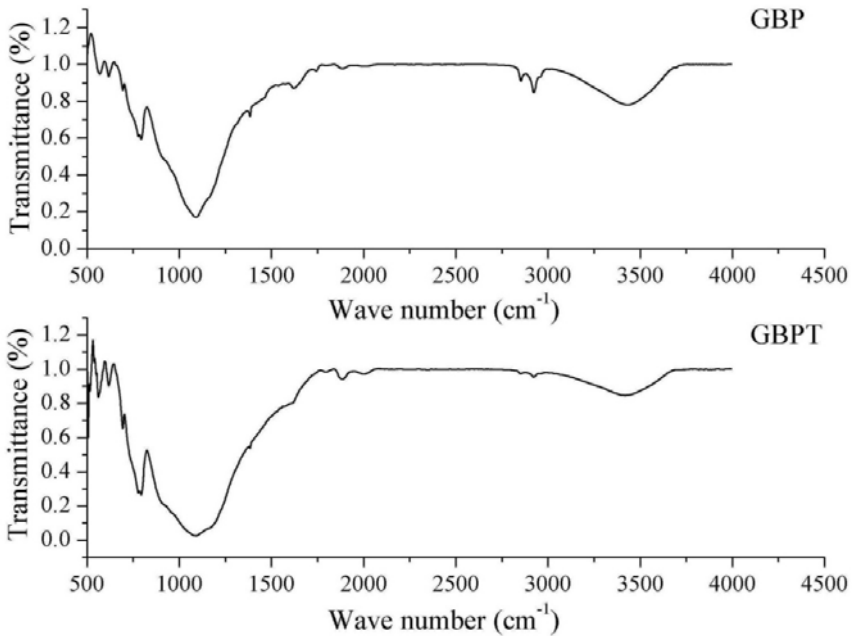

(a) Spectrum of GBP before adsorption (GBP) and after adsorption (GBPT)

Fig. 1 FTIR spectrum of adsorbent: (a) GBP; (b) RS

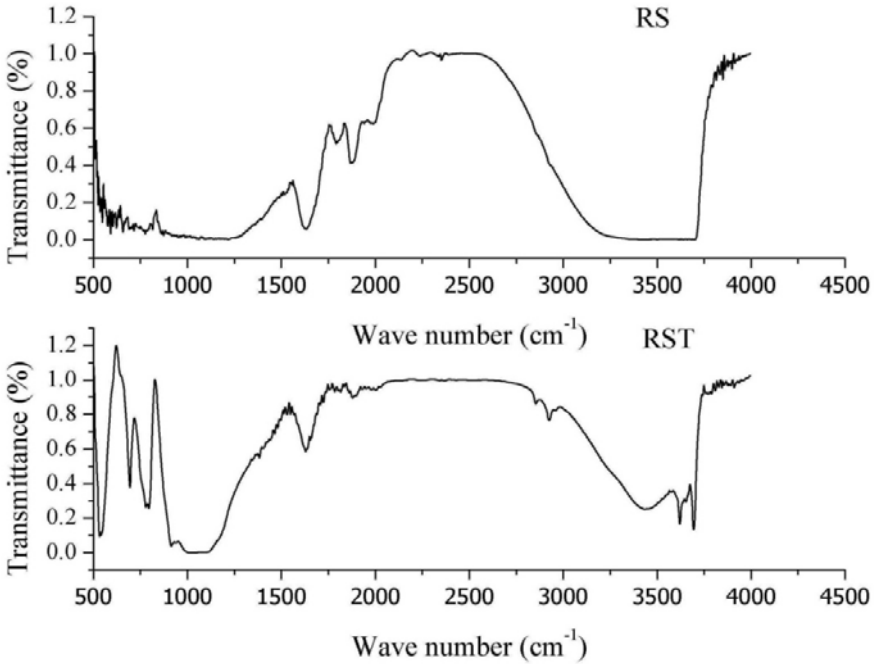

(b) Spectrum of RS before adsorption (RS) and after adsorption (RST)

Fig. 1 Continued

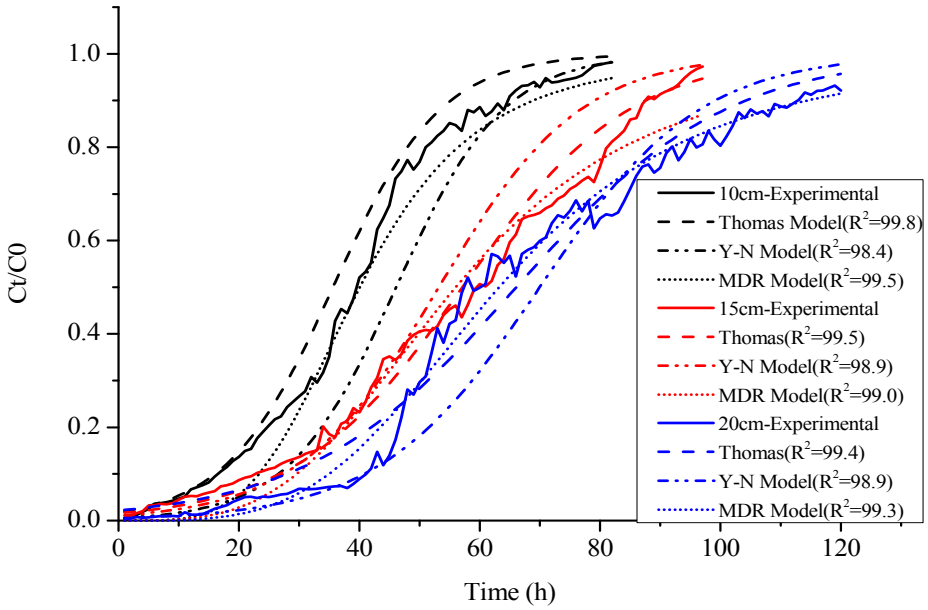

Fig. 2 Breakthrough curves from experiments (———) and models (— — —) at different bed heights (Q = 5 mL/min, C_0 = 15 mg/L)

phosphate concentrations as discussed in the following paragraphs.

3.3.2 Effects of different bed heights

To investigate the effect of bed height on the breakthrough curve of the column adsorption process, bed heights were varied as 10, 15 and 20 cm with a constant flow rate of 5 mL/min and influent phosphate concentration of 15 mg/L. Fig. 2 shows the related breakthrough curves. It is clear from the figures that both the breakthrough and exhaustion times got extended from 13 to 21 to 27 h and 74 to 92 to 111 h, respectively, with increasing bed heights from 10 to 15 to 20 cm (Table 2). Subsequently, the volume of phosphate solution treated at breakthrough point and exhaust point was largest (Table 2) for longer bed heights as compared to shorter ones. This point outs that, the smaller beds get saturated sooner than the longer beds. This might be due to the longer bed height allowing a longer contact time between the adsorbent and the adsorbate. Also, with increase in bed heights, amounts of adsorbent increases, thereby resulting in availability of more active surfaces for adsorption. In addition, the slope of the breakthrough curves became flatter with increasing bed heights, as a consequence an expanded mass transfer zone formation took place (Nur *et al*. 2013). Therefore the columns with the longer adsorbent beds, apparently took a much longer time to reach complete exhaustion contributing to the higher service time of the beds.

3.3.3 Effects of different flow rates

The effect of flow rates on the breakthrough curve of the column adsorption process was assessed by varying the flow rates as 2.5, 5 and 7.5 mL/min while keeping the bed height 15 cm and initial phosphate concentration 15 mg/L. Fig. 3 shows that higher flow rate results in shorter column exhaustion time and steeper breakthrough curves. As the flow rate goes on increasing from

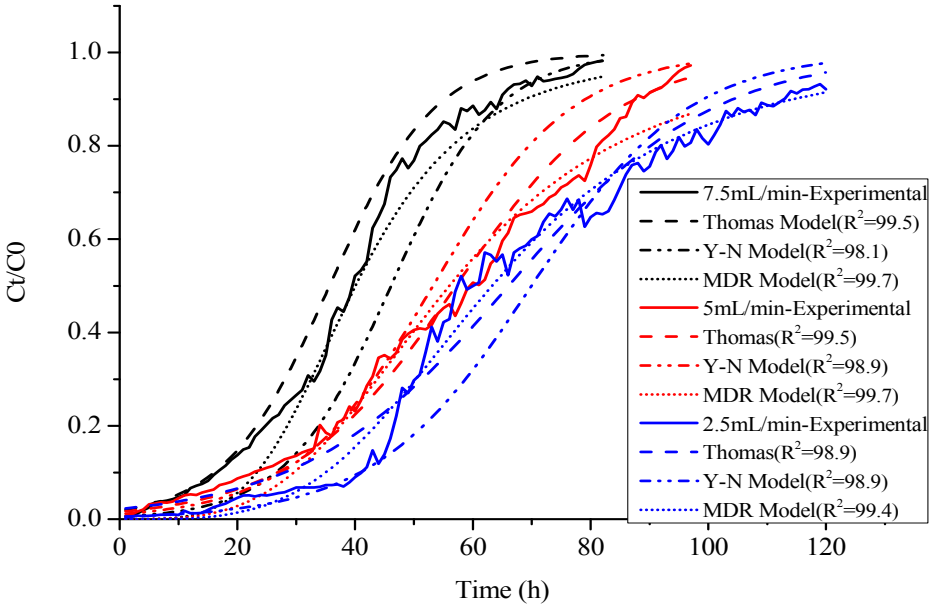

Fig. 3 Breakthrough curves from experiments (———) and models (— — —) at different flow rates (Bed height = 15 cm, C_0 = 15 mg/L)

2.5 to 5 to 7.5 mL/min, the respective break through and exhaustion time follows the reverse order from 44 to 21 to 11 h and 138 to 92 to 76 h. The EBCT decreased (Table 2) with the increased in the flow rate. So at lower flow rates, more residence time leads to more adsorbate-adsorbent interaction and higher diffusion of phosphates onto the adsorbents utilizing the maximal portion of the adsorbent bed. Thus, exhibits more longevity in performance of the column bed. On the other hand, higher flow rate results in lower residence time and generates high turbulence. The combinatorial effects of the latter two factors lead to a weaker adsorbate-adsorbent interaction and disturbs the intraparticle mass transfer between the phosphate ion and the adsorbent (Zhao *et al*. 2014). Hence saturation time decreases contributing to lesser longevity in column bed performance.

3.3.4 Effects of influent phosphate concentration

In order to investigate the effect of the influent phosphate concentration on the breakthrough curves, initial phosphate concentration was varied as 5 and 15 mg/L with constant flow rate of 5 mL/min and bed height of 15 cm. The resultant breakthrough curves are demonstrated in Fig. 4. It is evident from the figure that, at lower influent phosphate concentrations, breakthrough curves were flatter and breakthrough occurred slower as compared to the case of higher influent concentration, where steeper breakthrough curves and faster bed saturation were observed. With the increase of influent phosphate concentration from 5 to 15 mg/L, the respective break through and exhaustion time decreases from 34 to 21 h and 139 to 92 h respectively. As a matter of fact the volume of phosphate solution treated at breakthrough point and exhaust point as shown in Table 2 (10.2 and 41.7 L) for 5 mg/L phosphate concentration were more than that of the respective volumes (6.3 and 27.6 L) of 15 mg/L phosphate concentrations. This can be explained on the basis

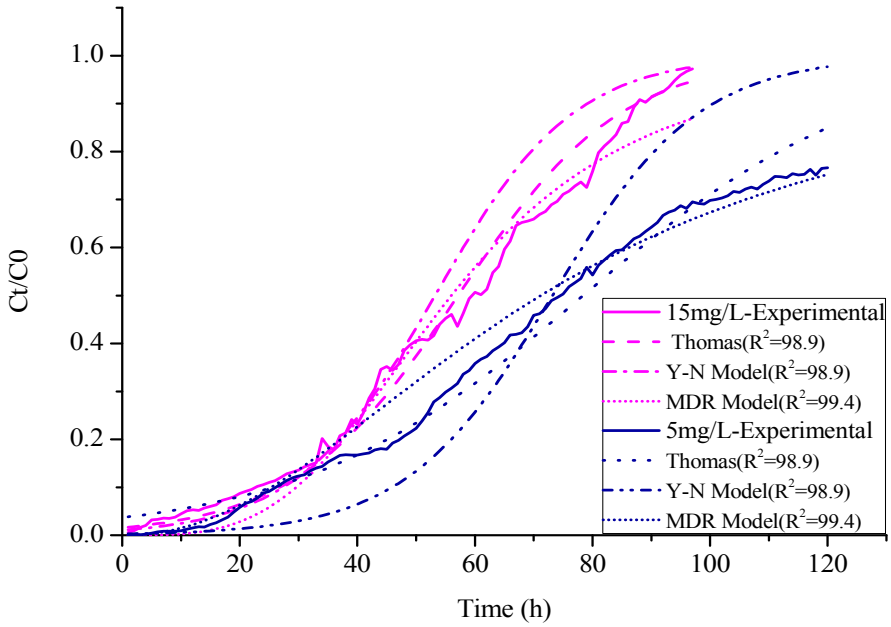

Fig. 4 Breakthrough curves from experiments (———) and models (— — —) at different influent phosphate concentrations (Bed height = 15 cm, Q = 5 mL/min)

Table 2 Parameters and column data for fixed bed column phosphate adsorption

L (cm)	Q (L/h)	C_0 (mg/L)	t_b (h)	t_e (h)	V_b (L)	V_e (L)	MTZ (cm)	U_z (cm/h)	$EBCT$ (min)	q_e (mg/g)	(%) Bed saturation*
10	0.3	15	13	74	3.9	22.2	8.24	0.135	31.8	1.994	20.45
15	0.3	15	21	92	6.3	27.6	11.57	0.163	47.7	1.704	25.39
20	0.3	15	27	111	8.1	33.3	15.13	0.180	63.6	1.518	27.05
15	0.15	15	44	138	6.6	20.7	10.21	0.109	95.4	1.278	34.62
15	0.3	15	21	92	6.3	27.6	11.57	0.163	47.7	1.704	25.39
15	0.45	15	11	76	4.95	34.2	12.82	0.197	31.8	2.112	17.8
15	0.3	5	34	139	10.2	41.7	11.33	0.108	47.7	0.858	32.82
15	0.3	15	21	92	6.3	27.6	11.57	0.163	47.7	1.704	25.39

*The percentage of the total column saturated at breakthrough

that, intraparticle diffusion controls adsorption process, and diffusion process is concentration dependent. Therefore a change in concentration gradient affects the breakthrough time as well as saturation rate. Higher initial influent concentrations resulted in higher driving force to overcome the mass transfer resistance; therefore the adsorbent column achieved saturation more rapidly, resulting in quick exhaustion of the bed (Nur *et al*. 2013). Whereas the lower initial concentration of phosphate caused slower diffusion of phosphate onto the adsorbent due to decreased mass transfer coefficient, thereby contributing to the lengthier exhaustion time of the column (Uddin *et al*. 2009).

3.3.5 Mechanism of phosphate removal

As discussed earlier in Section 3.1, phosphate removal occurs either via ligand exchange forming inner-sphere complexes or via precipitation. Hydrolysis of metal oxides generate metal cation and hydroxyl anion (OH^-) as per the following equation.

$$M_aO_b + b\mathrm{H_2O} \rightarrow aM\left(2b/a\right)^+ + 2b\mathrm{OH}^- \tag{12}$$

$$M\left(2b/a\right)^+ \ldots\ldots\ldots \mathrm{H_2PO_4^-} \tag{13}$$

The cationic species participates in phosphate up taking through electrostatic interaction, whereas the anionic species is used in inner-sphere ligand exchange mechanism. Similarly phosphate metal precipitation occurs as per the equation given below

$$3M^{(a)+}aPO_4^{3-} = M_3\left(PO_4\right)a \tag{14}$$

3.4 Modelling of column adsorption data

Successful design of a fixed bed column adsorption process required accurate generation of breakthrough curves and prediction of concentration-time profile for the effluent. Kinetic models were essential to predict the dynamic behavior of fixed bed column adsorption process. In this study, to predict and analyze the process of phosphate adsorption onto a mixture of RS and GBP,

used as adsorbents in a fixed- have not only been able to describe the breakthrough curves more accurately, but also provide bed column, four kinetic models, namely, BDST, Thomas, Yoon-Nelson (Y-N) and Modified Dose Response (MDR) models were applied to experimental data. The linear regression method was followed for BDST model, whereas non linear regression was opted for the other three models. These models important system parameters that can be utilized to scale-up fixed bed column adsorption processes. The co-efficient of correlation (R^2) and the sum of the squares of the errors (SSE) were used to describe the fit of the experimental and predicted data and to predict the best fit models.

3.4.1 Analysis of adsorption data by Bed Depth Service Time (BDST) model

BDST is the most basic and widely used model used to predict the column performance for any bed length, if data for some depths are known. BDST model constants can be used to scale up the height of the adsorption column beds for given inlet adsorbate concentration. The model constants are further helpful to scale up the process for other concentrations and flow rates without further experimental runs. The model is based on the supposition that the rate of adsorption is regulated by the surface interaction between the adsorbate and the unused adsorbent. The main design criteria focus on predicting the service time of the bed, where service time is nothing but the time taken by the adsorbent to remove a specific amount of adsorbate from the solution before the requirement of regeneration. The model states that, there exists a linear relationship between bed height (L) and service time (t) as given by Eq. (15): (Hutchins 1973)

$$t = \frac{N_0 L}{C_0 U} - \frac{1}{K_\alpha C_0} \ln\left(\frac{C_0}{C_b} - 1\right) \tag{15}$$

where, C_0 is the initial dye concentration (mg/L), C_b is the breakthrough dye concentration (mg/L), U is the linear velocity (cm/h), t is the time (h) and L is the bed height (cm) of the column, N_0 is the adsorption capacity of the bed (mg/L), K_α is the rate constant in BDST model (L/mg/h). A plot of t versus L yielded a linear relationship as shown in Fig. 5. N_0 and K_α were evaluated from the slope and intercept of the plot respectively. N_0 and K_α values for breakthrough point and exhaustion point are 1.4, -0.67 and 3.7, 36.84 respectively.The bed capacity (N_0), mostly changes with time. With the increase in the bed depth, the residence time of the fluid inside the column increases, allowing the adsorbate molecules to adsorb more onto the adsorbent, thereby changing the bed capacity with the service time. K_α basically signifies the rate of transfer of solutes from liquid phase to the solid phase. The larger the K_α value more is the performance efficiency of the bed (Uddin *et al*. 2009). The higher value of K_α (36.84) for exhaustion point straightforwardly indicates more service time for the same. Moreover, the R^2 value for breakthrough point (0.986) and for exhaustion point (0.999) indicate that the fixed column phosphate adsorption process is valid according to BDST model.

3.4.2 Analysis by Thomas Model

The maximum adsorption capacity of an adsorbent (q_m) is an unavoidable design parameter of an adsorbent column. Thomas model is one of the most general and widely used model to describe the adsorption process, the maximum solid phase concentration adsorbate on adsorbent and the adsorption rate constant in fixed bed column mode operation. The model is based on the following assumption: the rate driving force follows second-order reversible reaction kinetics, there is no axial dispersion and Langmuir kinetics of adsorption/desorption. This model can be used well,

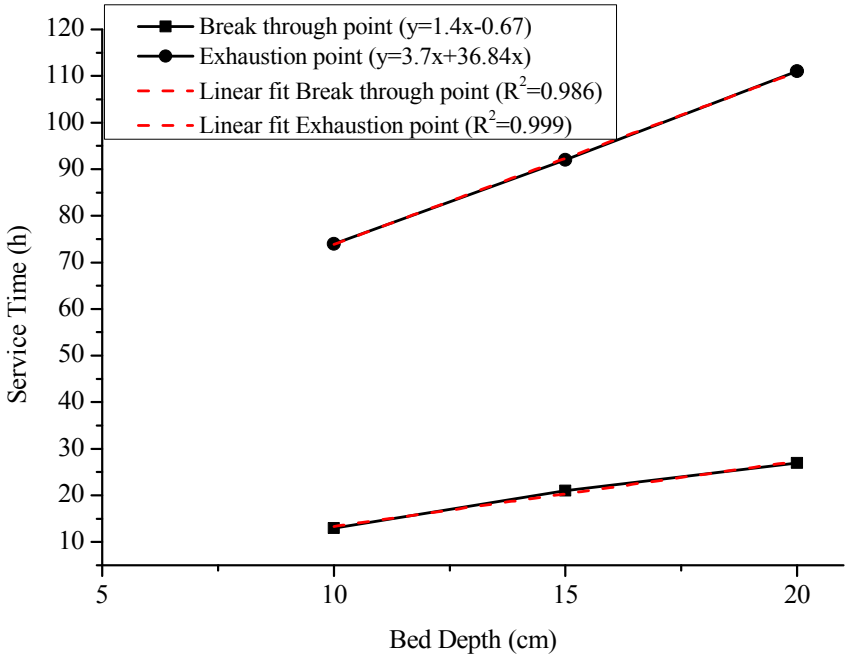

Fig. 5 BDST model for different bed heights (Q = 5 mL/min, C_0 = 15 mg/L)

especially in the absence of internal and external diffusion limitation (Thomas 1944). The form of Thomas model is as follows

$$\frac{C_t}{C_0} = \frac{1}{1+\exp\left[\frac{K_t}{Q}\left(q_m m - C_0 V\right)\right]} \tag{16}$$

where, K_t is the Thomas rate constant (L/h mg), q_m is the maximum solid phase concentration of the solute (mg/g), V is the effluent volume (L), m is the mass of adsorbent (g), and Q is the flow rate (L/h).

In this study, still a simpler form of the Thomas model as represented in Eq. (17) (Aksu and Gonen 2004) was applied to the column adsorption experimental data at different operating conditions.

$$\frac{C_t}{C_0} = \frac{1}{1+\exp\left[A - Bt\right]} \tag{17}$$

where, A and B are constants of Thomas model and the value of t, is flow time (min). Model fitting was done by nonlinear regression analysis and the predicted curves at various experimental conditions, according to the Thomas model are shown in Figs. 2-4. The Thomas model parameters as per Eq. (17), the values of R^2 and SSE at different operating conditions are all listed in Table 3. It is observed from Table 3 that the values of A increased with the increase of bed height, and influent phosphate concentration. Also, first increased followed by decreased with an increase in flow rate. Whereas the values of B decreased with increase in bed heights, increased with an

Table 3 Parameters of Thomas model and values of R^2 and SSE at different conditions

L (cm)	Q (L/h)	C_0 (mg/L)	a	b	R^2	SSE
10	0.3	15	3.79	0.087	0.998	0.000357
15	0.3	15	4.13	0.072	0.995	0.0045
20	0.3	15	4.97	.065	0.994	0.0037
15	0.15	15	3.8	.0576	0.989	0.0027
15	0.3	15	4.13	0.72	0.995	0.0045
15	0.45	15	3.99	0.112	0.995	0.00054
15	0.3	5	3.26	.041	0.988	0.0028
15	0.3	15	4.13	0.72	0.995	0.0045

increase in influent phosphate concentration and first increased followed by decreased with an increase in the flow rate. The values of R^2 range from 0.988 to 0.998 while the values of SSE range from 0.0027 to 0.00054. The high values of R^2 and low values of SSE, demonstrated the goodness of fit between the experimental data and corresponding predicted values by Thomas model. Furthermore, the Figs. 2-4 clearly show how the Thomas model suitably describes the adsorption of phosphates by GBP and RS mixture used as adsorbent in fixed bed column adsorption mode.

3.4.3 Analysis by Yoon-Nelson (Y-N) Model

Yoon-Nelson model (Yoon and Nelson 1984), one of the simplest kinetic model is used to predict the exhaustion time and the behavior of adsorption process for a given adsorbate concentration. This model is based on the assumption that the rate of de-crease in the probability of adsorption for each adsorbate molecule is directly proportional to the probability of the adsorbate molecule adsorption and the adsorbate breakthrough on the adsorbent. This model necessitates no detailed data regarding physiochemical properties of adsorbate and adsorbent. The mathematical expression of the model is given in Eq. (18)

$$\frac{C_t}{C_0} = \frac{\left(\exp(K_Y t) - \tau K_Y\right)}{1 + \left(\exp(K_Y t) - \tau K_Y\right)} \tag{18}$$

where, K_Y Is the Yoon-Nelson rate constant (1/h), and τ (h) is the time required for 50% breakthrough point. In this study, in order to predict the breakthrough behavior of the fixed bed column, the nonlinear regression fitting of the experimental data to the Yoon–Nelson model as per Eq. (18) was done. The predicted breakthrough curves by the Yoon-Nelson model, together with the analogous experimental data, are shown in Figs. 2-4. The Yoon-Nelson model parameters and the values of R^2 and SSE at different operating conditions were all listed in Table 4. The high values of R^2 (0.981-0.989) and low values of SSE (0.0003-0.180) as given in the Table 4 advocated that Yoon-Nelson model fitted well to the experimental data of this study. As shown in Table 4, the K_Y values decreased, but τ increased with increasing bed depth. On the other hand, with increased in flow rate and influent phosphate concentration the values of 50% breakthrough time (τ) decreased but the value of K_Y increased. Significant decrease in τ value with decreased bed

Table 4 Parameters of Yoon-Nelson model and values of R^2 and SSE at different conditions

L (cm)	Q (L/h)	C_0 (mg/L)	K_Y (1/h)	T (h)	R^2	SSE
10	0.3	15	0.889	51.12	0.984	0.0003
15	0.3	15	.085	53.23	0.989	0.0055
20	0.3	15	.063	59.22	0.989	0.011
15	0.15	15	.075	69.97	0.989	0.180
15	0.3	15	.085	53.23	0.989	0.0055
15	0.45	15	0.112	46.11	0.981	0.0005
15	0.3	5	0.80	73.19	0.987	0.034
15	0.3	15	.085	53.23	0.989	0.0055

height, increased inflow velocity and increased influent phosphate concentration is attributed to rapid saturation of fixed bed columns. Similar types of association between a decrease of τ and an increase of K_Y with the increased in flow rate and influent adsorbate concentration were reported by earlier researchers (Yaghmaeian *et al*. 2014, Chen *et al*. 2012).

3.4.4 Analysis by Modified Dose Response (MDR) Model

Another simplified numerical model used to describe fixed bed column adsorption data is the Modified Dose Response model (Yan *et al*. 2001). This model basically diminishes the error resulting from the use of the Thomas model, particularly at lower or higher time periods of the breakthrough curve. The mathematical expression of the model is represented as below

$$\frac{C_t}{C_0} = 1 - \frac{1}{1 + \left(V_t / b\right)^a} \tag{19}$$

where, a and b are Modified Dose Response model constants. From the value of b, the value of the maximum solid phase concentration of the solute (q_m) can be anticipated by using the following equation

$$q_m = \frac{bC_0}{m} \tag{20}$$

Nonlinear regression method was followed to fit the experimentally obtained data into the Modified Dose Response model as given in Eq. (20). The experimental along with predicted breakthrough curves are shown in Figs. 2-4 and the relevant constants, R^2 and SSE values are presented in Table 5. It is evident from the figure as well as strikingly high R^2 (0.993-0.997) and low SSE (0.0004-0.0021), that the predicted breakthrough curves of the Modified Dose Response model exemplify an excellent concurrence with the experimental plots at all conditions experimented. It is clear from Table 5, that the values of b increased with the increase in bed depth and flow rate as well. But it became smaller with the increase of influent phosphate concentration. Values were increased with an increase in influent phosphate concentration, but there was no particular trend observed in the case of increase in bed height and flow rate. Similar type of finding was also reported by Zhao *et al*. (2014).

Table 5 Parameters of Modified Dose Response model and values of R^2 and SSE at different conditions

L (cm)	Q (L/h)	C_0 (mg/L)	a	b	R^2	SSE
10	0.3	15	3.75	12.45	0.995	0.0014
15	0.3	15	3.44	16.79	0.99	0.0021
20	0.3	15	4.72	18.39	0.993	0.0008
15	0.15	15	3.7	9.48	0.994	0.0012
15	0.3	15	3.44	16.79	0.99	0.0021
15	0.45	15	4.05	18.03	0.997	0.0013
15	0.3	5	2.12	21.35	0.994	0.0004
15	0.3	15	3.44	16.79	0.99	0.0021

3.4.5 Comparison of applied numerical models

The correlation coefficient (R^2) and Sum of the Square of the Errors (SSE) were used to establish the best fit model out of Thomas, Yoon-Nelson (Y-N) and Modified Dose Response (MDR) models. As per the data listed in Table 3-5, the range of values of R^2 from Modified Dose Response model (0.993-0.997) were the highest, followed by the Thomas and Yoon-Nelson model with respective values of 0.988-0.998 and 0.981-0.989 at the same experimental condition. Similarly the values of SSE from MDR model (0.0004-0.0021) were lower than that of Thomas (0.0027-0.00054) and Y-N (0.0003-0.180) models. Thus, it was inferred that the MDR model was better in describing the process of phosphate adsorption by a mixture of RS and GBP than that of Thomas and Y-N model. If we will have a close look at the curves shown in Figs. 2-4, it can be clearly seen that fitted curves of MDR model were better close to the experimental curves than that of the curves of Thomas and Y-N model. The results depict that all the models exhibit very high correlation coefficient (> 0.98), means all the three models can suitably predict the fixed bed column adsorption process. The best fitting of the models to the experimental data will follow the order as: MDR > Thomas > Y-N. The comparison between R^2 and SSE values of the MDR and Thomas model of this study is in agreement with the findings of Yan *et al*. (2013).

3.5 Desorption and reusability of adsorbent

After the fixed bed column got saturated, it was subjected to desorption in order to regenerate the adsorbent for subsequent reuse. In this study, the desorption process was carried out by passing 0.1M HCl through the saturated bed at a filtration velocity of 0.5 L/h for 2 h. Fig. 6 shows the results of the adsorption and desorption cycles, which were repeated up to 3 times. The phosphate adsorption and desorption in 1st cycle was found to be 94 and 87%. But after 3rd cycle the corresponding values were reported to be 78.5 and 70.2% respectively. The results demonstrated that both the adsorption and desorption capacity of the adsorbent were maintained well above 80% of the original capacity in the 3rd cycle, indicating the reusability potential of the adsorbent. The capacity loss by increasing the number of adsorption/desorption cycle is attributed to the occupancy of some of the active sites of the adsorbent by the non-desorbed phosphates and the destruction of the layered structure of the adsorbent. In spite of the high rate of desorption, the process is not encouraged in this study since: (i) GBP and RS are copiously available respectively, as waste and natural materials; (ii) desorption process incurred some cost as 0.1M HCl is being

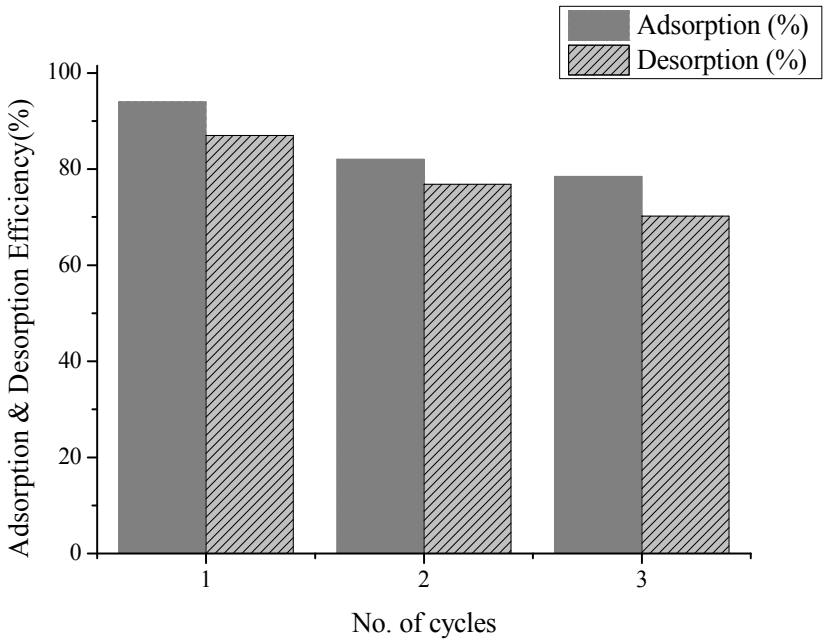

Fig. 6 Efficiency of the adsorption / desorption cycle

used for the same; and (iii) applicability of phosphate enriched GBP and RS mixture in agricultural fields for serving the purpose of phosphate availability to plants and enhanced hydraulic conductivity.

4. Conclusions

This mixture of GBP and RS is found to be a promising cost effective adsorbent for the removal of phosphate from aqueous solution. The experimental data revealed that an increase in bed height and initial phosphate concentration or a decrease of flow rate enhances the longevity of column performance by increasing both breakthrough time and exhaustion time thereby delaying bed saturation. Overall exhaustion time for the column in various experimental conditions were found to be quite high with a range of 72-139 h. The BDST model with a perfect linear plot (R^2 > 0.98) suitably predicts the breakthrough curve. With very high correlation coefficient (> 0.98) all the three nonlinear models, e.g., Thomas, Yoon-Nelson and Modified Dose Response were found to fit well to the column adsorption data. The best fitting of the models to the experimental data followed the order as: Modified Dose Response > Thomas > Yoon-Nelson. The results of this finding also reflected the concurrency with the theory that the use of Modified Dose Response model minimizes the error resulting from the use of the Thomas model. Exploring the adsorption/desorption capacity of the mixture of adsorbents revealed that, the capacity was not significantly reduced after 3 successive adsorption/desorption cycles. Therefore the adsorbent mixture is appropriate for a continuous system. Moreover the phosphate rich spent adsorbent can find its applicability in agricultural fields for serving the purpose of phosphate availability to plants and enhanced hydraulic conductivity. Therefore, we concluded that the results of the study

support the use of a mixture of GBP and RS as potential adsorbents for phosphate removal from aqueous solution in continuous flow through systems.

Acknowledgments

The authors are thankful to School of Infrastructure, Indian Institute of Technology Bhubaneswar, India, for providing facilities to carry out the research work in the concerned area.

References

Adak, A., Bandyopadhyay, M. and Pal, A. (2006), "Fixed bed column study for the removal of crystal violet (C. I. Basic Violet 3) dye from aquatic environment by surfactant-modified alumina", *Dyes. Pigments.,* **69**(3), 245-251.

Aksu, Z. and Gonen, F. (2004), "Biosorption of phenol by immobilized activated sludge in a continuous packed bed: prediction of breakthrough curves", *Process Biochem.*, **39**(5), 599-613.

APHA, AWWA, WPCF (2005), *Standard Methods for the Examination of Water and Wastewater*, (21st Ed.), American Public Health Association, Washington DC, USA.

Cavas, L., Karabay, Z., Alyuruk, H., Dogan, H. and Demir, G.K. (2011), "Thomas and artificial neural network models for the fixed-bed adsorption of methylene blue by a beach waste Posidonia oceanica (L.) dead leaves", *Chem. Eng. J.*, **171**(2), 557-562.

Chen, J.G., Kong, H.N., Wu, D.Y., Chen, X.C., Zhang, D.L. and Sun, Z.H. (2007), "Phosphate immobilization from aqueous solution by fly ashes in relation to their composition", *J. Hazard. Mater.*, **39**(2), 293-300.

Chen, S., Yue, Q., Gao, B., Li, Q., Xu, X. and Fu, K. (2012), "Adsorption of hexavalent chromium from aqueous solution by modified corn stalk: A fixed-bed column study", *Bioresour. Technol.*, **113**, 114-120.

Chen, H., Zhang, H. and Yan, Y. (2013), "Adsorption dynamics of toluene in structured fixed bed with ZSM-5 membrane/PSSF composites", *Chem. Eng. J.*, **228**, 336-344.

Jia, C.R., Dai, Y.R., Chang, J.J., Wu, C.Y., Wu, Z.B. and Liang, W. (2013), "Adsorption characteristics of used brick for phosphorous removal from phosphate solution", *Desalin. Water Treat.*, **51**(28-30), 5886-5891.

Chimenos, J.M., Fernandez, A.I., Villalba, G., Segarra, M., Urruticoechea, A., Artaza, B. and Espiella, F. (2003), "Removal of ammonium and phosphates from wastewater resulting from the process of cochineal extraction using MgO-containing by-product", *Water Res.*, **37**(7), 1601-1607.

Elzinga, E.J. and Sparks, D.L. (2007), "Phosphate adsorption onto hematite: An in situ ATR-FTIR investigation of the effects of pH and loading level on the mode of phosphate surface complexation", *J. Colloid. Interf. Sci.*, **308**(1), 53-70.

Huang, W., Li, D., Zhu, Y., Xu, K., Li, J., Han, B. and Zhang, Y. (2013a), "Phosphate adsorption on aluminum-coordinated functionalized macroporous–mesoporous silica:Surface structure and adsorption behavior", *Mater. Res. Bull.*, **48**(12), 4974-4978.
DOI: http://dx.doi.org/10.1016/j.materresbull.2013.04.093

Huang, W.Y., Zhu, R.H., He, F., Li, D., Zhu, Y. and Zhang, Y.M. (2013b), "Enhanced phosphate removal from aqueous solution by ferric-modified laterites: Equilibrium, kinetics and thermodynamic studies", *Chem. Eng. J.*, **228**, 679-687.

Hutchins, R.A. (1973), "New method simplifies design of activated carbon systems", *Chem. Eng.*, **20**, 133-138.

Ioannou, Z., Dimirkou, A. and Ioannou, A. (2013), "Phosphate adsorption from aqueous solutions onto Goethite, Bentonite, and Bentonite-Goethite system", *Water Air Soil Pollut.*, **224**, 1374-1382.

Jia, Z., Wang, Q., Liu, J., Xu, L. and Zhu, R. (2013), "Effective removal of phosphate from aqueous solution

using mesoporous rodlike NiFe2O4 as magnetically separable adsorbent", *Colloids. Surf. A Physicochem. Eng. Asp.*, **436**, 495-503.
DOI: http://dx.doi.org/10.1016/j.colsurfa.2013.07.025

Johansson, L. and Gustafsson, J.P. (2000), "Phosphate removal using blast furnace slags and opoka-mechanisms", *Water Res.*, **34**(1), 259-265.

Kadam, A.M., Nemade, P.D., Oza, G.H. and Shankar, H.S. (2009), "Treatment of municipal wastewater using laterite-based constructed soil filter", *Ecol. Eng.*, **35**(7), 1051-1061.

Karageorgiou, K., Paschalis, M. and Anastassakis, G.N. (2007), "Removal of phosphate species from solution by adsorption onto calcite used as natural adsorbent", *J. Hazard. Mater.*, **139**(3), 447-452.

Kennedy, V.J., Augusthy, A., Varier, K.M., Magudapathy, P., Panchapakesan, S., Nair, K.G.M. and Vijayan, V. (1999), "Elemental analysis of river sediments by PIXE and PIGE", *Int. J. PIXE.*, **09**, 407-416.

Krishnan, K.A. and Haridas, A. (2008), "Removal of phosphate from aqueous solutions and sewage using natural and surface modified coir pith", *J. Hazard. Mater.*, **152**(2), 527-535.

Liana, A.R., Maria, L. and Caetano, P.S. (2010), "Adsorption kinetic, thermodynamic and desorption studies of phosphate onto hydrous niobium oxide prepared by the reverse microemulsion method", *Adsorption*, **16**(3), 173-181.

Lindsay, W.L. (1979), *Chemical Equilibria in Soils*, Wiley, New York, USA.

Mateus, D.M.R. and Pinho, H.J.O. (2010), "Phosphorous removal by expanded clay-six years of pilot-scale constructed wetlands experience", *Water. Environ. Res.*, **82**(2), 128-137.

Mateus, D.M.R., Vaz, M.M.N. and Pinho, H.J.O. (2012), "Fragmented limestone wastes as a constructed wetland substrate for phosphorous removal", *Ecol. Eng.*, **41**, 65-69.

Nur, T., Johir, M.A.H., Loganathan, P., Nguyen,T., Vigneswaran, S. and Kandasamy, J. (2013), "Phosphate removal from water using an iron oxide impregnated strong base anion exchange resin", *J. Ind. Eng. Chem.*, **20**(4), 1031-1037.
DOI: http://dx.doi.org/10.1016/j.jiec.2013.07.009

Rahaman, M.A., Ahsan, S., Kaneco, S., Katsumata, H., Suzuki, T. and Ohta, K. (2005), "Wastewater treatment with multilayer media of waste and natural indigenous materials", *J. Environ. Manage.*, **74**(2), 107-110.

Rout, P.R., Bhunia, P. and Dash, R.R. (2014a), "A mechanistic approach to evaluate the effectiveness of red soil as a natural adsorbent for phosphate removal from wastewater", *Desalin. Water. Treat.*
DOI: http://dx.doi.org/10.1080/19443994.2014.881752

Rout, P.R, Bhunia, P. and Dash, R.R. (2014b), "Modelling isotherms, kinetics and understanding the mechanism of phosphate adsorption onto a solid waste: Ground Burnt Pattie", *J. Environ. Chem. Eng.*, **2**(3), 1331-1342.

Sun, X.F., Imai, T., Sekine, M., Higuchi,T., Yamamoto, K. and Kanno, A. (2013), "Adsorption of phosphate using calcined Mg3–Fe layered 3 double hydroxides in a fixed-bed column study", *J. Ind. Eng. Chem.*, **20**(5), 3623-3630.
DOI: http://dx.doi.org/10.1016/j.jiec.2013.12.057

Thomas, H.C. (1944), "Heterogeneous ion exchange in a flowing system", *J. Am. Chem. Soc.*, **66**(), 1466-1664.
DOI: http://dx.doi.org/10.1021/ja01238a017

Uddin, Md.T., Rukanuzzaman, Md., Khan, Md.M.R. and Islam, Md.A. (2009), "Adsorption of methylene blue from aqueous solution by jackfruit (Artocarpus heteropyllus) leaf powder: A fixed-bed column study", *J. Env. Manag.*, **90**(11), 3443-3450.

Wang, Y., Gao, B.Y., Yue, W.W., Xu, X.M. and Xu, X. (2008), "Adsorption kinetics of phosphate from aqueous solutions onto modified corn residue", *Environ. Sci.*, **29**(3), 703-708.

Yaghmaeian, K., Moussavi, G. and Alahabadi, A. (2014), "Removal of amoxicillin from contaminated water using NH4Cl-activated carbon: Continuous flow fixed-bed adsorption and catalytic ozonation regeneration", *Chem. Eng. J.*, **236**, 538-544.

Yan, G., Viraraghavan, T. and Chen, M. (2001), "A new model for heavy metal removal in a biosorption column", *Adsorpt. Sci. Technol.*, **19**(1), 25-43.

Yang, J., Wang, S., Lu, Z.B. and Lou, S.J. (2009), "Converter slag-coal cinder columns for the removal of phosphorous and other pollutants", *J. Hazard. Mater.*, **168**(1), 331-337.
Yoon, Y.H. and Nelson, J.H. (1984), "Application of gas adsorption kinetics. Part 1. A theoretical model for respirator cartridge service time", *Am. Ind. Hyg. Assoc. J.*, **45**(8), 509-516.
Yuan, M., Carmichael, W.W. and Hilborn, E.D. (2006), "Microcystin analysis in human sera and 469 liver from human fatalities in Caruaru, Brazil", *Toxicon*, **48**(6), 627-640.
Zhang, L., Hong, S., He, J., Gan, F. and Ho, Y.S. (2011), "Adsorption characteristic studies of phosphorous onto laterite", *Desalin. Water Treat.*, **25**(1-3), 98-105.
Zhao, B., Shang, Y., Xiao, W., Dou, C. and Han, R. (2014), "Adsorption of Congo red from solution using cationic surfactant modified wheat straw in column model", *J. Env. Chem. Eng.*, **2**(1), 40-45.
Zheng, T.T., Sun, Z.X., Yang, X.F. and Holmgren, A. (2012), "Sorption of phosphate onto mesoporous γ-alumina studied with in-situ ATR-FTIR spectroscopy", *Chemistry Cent. J.*, **6**(1), 26-36.
Zong, E., Wei, D., Wan, H., Zheng, S., Xu, Z. and Zhu, D. (2013), "Adsorptive removal of phosphate ions from aqueous solution using zirconia-functionalizedgraphite oxide", *Chem. Eng. J.*, **221**, 193-203.

CC